

MEASUREMENT OF HYDROGEN SOLUBILITY AND DESORPTION RATE IN V-4Cr-4Ti AND LIQUID LITHIUM-CALCIUM ALLOYS* J.-H. Park, R. Erck, E.-T. Park, S. Crossley, and F. Deleglise (Argonne National Laboratory)

OBJECTIVE

The objective of this study is to develop an in-situ experimental method to determine the solubility and desorption rate of hydrogen in V-4Cr-4Ti and liquid lithium-calcium alloys at temperatures and hydrogen partial pressures in a magnetic fusion reactor.

SUMMARY

Hydrogen solubility in V-4Cr-4Ti and liquid lithium-calcium was measured at a hydrogen pressure of 9.09×10^{-4} torr at temperatures between 250 and 700°C. Hydrogen solubility in V-4Cr-4Ti and liquid lithium decreased with temperature. The measured desorption rate of hydrogen in V-4Cr-4Ti is a thermally activated process; the activation energy is 0.067 eV. Oxygen-charged V-4Cr-4Ti specimens were also investigated to determine the effect of oxygen impurity on hydrogen solubility and desorption in the alloy. Oxygen in V-4Cr-4Ti increases hydrogen solubility and desorption kinetics. To determine the effect of a calcium oxide insulator coating on V-4Cr-4Ti, hydrogen solubility in lithium-calcium alloys that contained 0-8.0 percent calcium was also measured. The distribution ratio R of hydrogen between liquid lithium or lithium-calcium and V-4Cr-4Ti increased as temperature decreased ($R \approx 10$ and 100 at 700 and 250°C , respectively). However at $<267^\circ\text{C}$, solubility data could not be obtained by this method because of the slow kinetics of hydrogen permeation through the vanadium alloy.

INTRODUCTION

The hydrogen ion density for fusion reactor designs is $1.2 \times 10^{20}/\text{m}^3$, which corresponds to a pressure of 10^{-5} torr at room temperature. Interaction between hydrogen and first-wall components may not be a significant concern for hydrogen embrittlement of structural materials because of the low density of hydrogen. However, for the design of a liquid-metal cooling system for fusion-reactor blanket applications, it is important to determine the solubility and transport kinetics of hydrogen in the structure and coolant. This study focused on developing methods for in-situ measurement of the solubility of hydrogen in vanadium-base alloys and liquid lithium. Initial results were presented in a previous report [1]. To investigate the effect of oxygen impurity in the vanadium alloy, oxygen-charged samples were tested in addition to those that were used previously [2]. The rate of hydrogen penetration into vanadium and its alloys is among the highest for metals [3-7]. Currently, we are proposing a calcium oxide insulator coating for magnetic-fusion-reactor (MFR) applications because of its a high thermodynamic stability and electrical resistivity [8]. Therefore this study has been extended to include liquid lithium with calcium and calcium oxide.

EXPERIMENTAL PROCEDURES

Sample Preparation

V-4Cr-4Ti. Small tabular-shaped samples of V-4Cr-4Ti (Table 1) were used in the investigation. To determine the oxygen impurity effect, several samples were charged with oxygen by exposure to high-purity argon (99.999%) at 625-650°C for 17 h [2]. Samples were weighed before and after oxygen charging. Typical depth of the oxygen enriched layer was 25 μm , which was determined from back-scattered-electron images obtained in a scanning electron microscope and from microhardness profiles of specimen cross sections.

* Work supported by Office of Fusion Energy, U.S. Department of Energy, under Contract W-31-109-Eng-38.

Li and Li-Ca alloys. Approximately 1.3 g of liquid lithium was loaded (Table 2) into a V-7.5Cr-15Ti tube (7.5-mm diameter, 0.4-mm wall thickness, 128.5-mm long, and 6.8289 g) with V-20Ti end plugs (7-mm long, 2.313 g). Small amounts of calcium were added in some experiments. After loading the lithium and lithium-calcium, the tube was sealed by tungsten inert gas (TIG) welding in a helium gas environment. To check for leakage, individual sealed cells were heated in a vacuum chamber at 700°C for 24 h. None of the cells leaked. The cells were cleaned by heating during the leak testing procedure, and after cooling, the outside of the cells was sputter-coated with palladium to avoid surface contamination during hydrogen desorption measurements.

Table 1. Description of samples and experimental procedures

Item Code	Sample wt. (g)	Sample Area (mm ²)	Data No. Code	Materials and Shape	Obtainable Parameters and Calculation	Notes
A			1-6 12-16	Ta tube furnace (178 mm long x 12.7 mm dia. x 0.5 mm thick)	Background for desorption and solubility	
B	21.89	28.68	7-11 17-21 28 41-43	A + V-4Cr-4Ti bar (101.3 x 10.15 x 3.64 mm)	Desorption rate and solubility (B-A)	Solubility and desorption rate in V-4Cr-4Ti
C	10.0	35.4	47-50	A + V-4Cr-4Ti (128.3 x 12.7 x 1 mm)	Desorption rate and solubility (C-A)	Solubility and desorption rate in V-4Cr-4Ti
D	23.5	90.57	44-46 51	A + C + V-4Cr-4Ti: (128.3 x 6.65 x 1 mm) and (128.3 x 12.7 x 1 mm)	Desorption rate and solubility (D-C) or (D-A)	Solubility and desorption rate in V-4Cr-4Ti
E	-	-	22-25 27	A + V-7.5Cr-15Ti (two plugs)	Background for Liquid-Li (+Ca) solubility	Base for solubility
F	-	31.16	29-32 37-40	A + Cell 2 (Li)	Solubility (F-E)	Solubility in Li
G	-	31.16	33-36	A + Cell 4 (Li+Ca)	Solubility in Li-Ca (G-E), (G-F)	Solubility effect of Ca in Li
H	-	31.16	88-91	A + Cell 1 (Li+Ca)	Solubility (H-E), (H-F), (H-G)	Effect of CaO layer

Table 2. Amount of lithium and calcium loaded in V-7.5Cr-15Ti tubes

V-7.5Cr-15Ti Tube	Li (g)	Ca (g)	wt.% Ca in Ca-Li	Mole fraction Ca in Ca-Li
Cell 1 ^a	1.23	0.07	5.4	9.78×10^{-3}
Cell 2	1.34	none	0.0	0.0
Cell 3 ^b	1.27	0.01	0.78	1.36×10^{-3}
Cell 4	1.29	0.11	7.86	1.46×10^{-2}

^aCell 1 was oxygen-charged in 99.999% argon and had a CaO coating on the inside wall (Ref. 2).

^bCell 3 was not tested.

Instrumentation and Method

Hydrogen charging and the desorption procedures and parameters (e.g., volume of the vacuum chamber, steady-state flow rate vs. residual pressure) were described in a previous report [1]. Figure 1 is a schematic drawing of the apparatus.

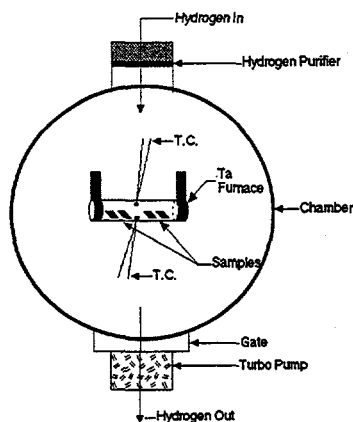


Figure 1.
Schematic drawing of the apparatus

RESULTS AND DISCUSSION

V-4Cr-4Ti

Desorption experiment. Figure 2 (a) shows the integral amount of hydrogen evolved at 518°C during degassing of an oxygen-charged V-4Cr-4Ti specimen after exposure to hydrogen for 1, 5, and 18 h and for an as-received V-4Cr-4Ti specimen after a 30 h exposure to hydrogen; Fig. 2 (b) shows hydrogen desorption rates during degassing of the specimens at these times. During degassing experiments at higher temperature, the specimen was held at 518°C for 2 min before heating to a higher temperature (850°C), at which the amount of degassed hydrogen was monitored by hydrogen pressure and the calculated flow rate, which was integrated with time to obtain solubility data as described previously [1].

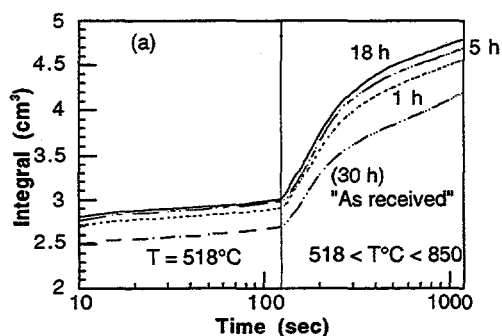


Figure 2(a).
Integral amount of hydrogen evolved during degassing of oxygen-charged V-4Cr-4Ti at 518°C after exposure to hydrogen for 1, 5, and 18 h and of as-received V-4Cr-4Ti after hydrogen charging for 30 h

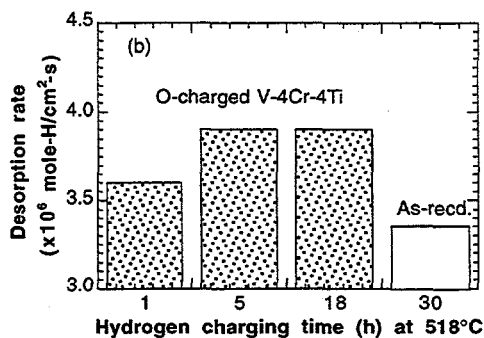


Figure 2(b).
Desorption rates of hydrogen from oxygen-charged V-4Cr-4Ti at 518°C after hydrogen-charging for 1, 5, and 18 h, and for as-received V-4Cr-4Ti after 30 h

Oxygen in V-4Cr-4Ti increases both the hydrogen solubility and desorption kinetics, as shown in Fig. 2. When we examine the degassing data at 518°C in Fig. 2 (b), initially (0 - 2 min), the integrated hydrogen desorption is higher for the oxygen-charged sample. The degassing process at 518°C showed a slight difference in the amount of hydrogen evolved from the specimen at 5 and 18 h. This means that a 1-mm-thick oxygen-charged V-4Cr-4Ti specimen is not equilibrated in 5 h. Therefore, the diffusivity of hydrogen (D_H) in oxygen-charged V-4Cr-4Ti at 518°C should be $D_H \leq 5.56 \times 10^{-7} \text{ mm}^2/\text{s}$, a value that is similar to the value for the as-received samples and much lower than literature values [5,6]. To resolve this difference, more effort will be required to analyze the degassing of components in the apparatus by mass spectroscopy with a residual-gas analyzer. Figure 4 shows the temperature dependence of the hydrogen desorption rate obtained from the difference of curves C and D in Fig. 3. Figure 5 shows the Vickers hardness-versus-depth profile for as-received, oxygen-charged, and an oxygen-charged sample equilibrated with hydrogen at 518°C. The decrease in hardness near the surface of the hydrogen-equilibrated sample indicates that, during the degassing process, oxygen was also removed to a depth of $\approx 8 \mu\text{m}$, as shown in Fig. 5. The measured desorption rate of hydrogen in V-4Cr-4Ti is a thermally activated process and the activation energy is 0.067 eV. However, more work is needed to determine the dependence of D_H on microstructure, as shown for nickel in Ref. 9.

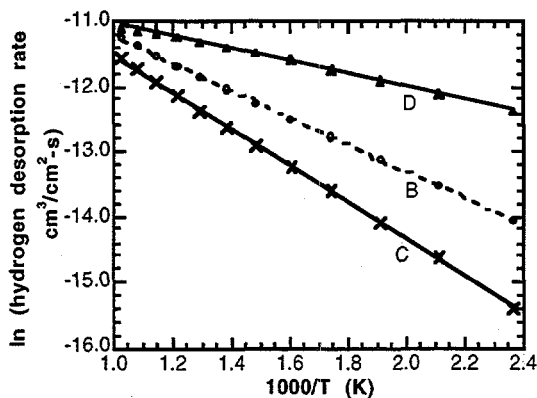


Figure 3. Hydrogen desorption rate vs. reciprocal temperature for V-4Cr-4Ti. B, C, and D denote the Item Code in Table 1.

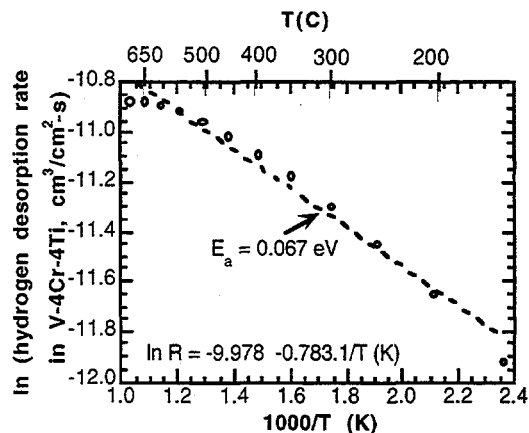


Figure 4. Hydrogen desorption rate vs. reciprocal temperature for V-4Cr-4Ti. Data obtained by taking the difference between C and D in Fig. 3.

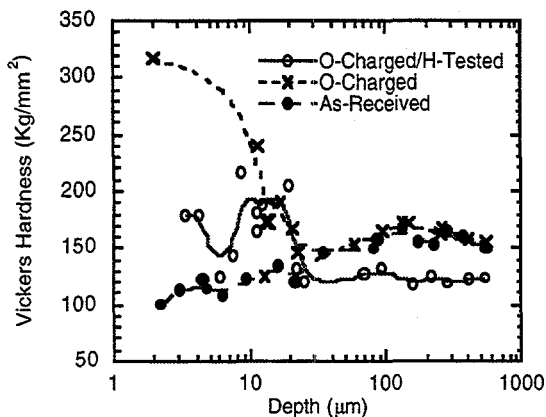


Figure 5. Vickers hardness-vs.-depth profiles for as-received and oxygen-charged samples, and oxygen-charged samples after hydrogen charging

Li or Li-Ca

Solubility measurement. Solubility was determined according to item codes F-H in Table 1. Figure 6 indicates typical hydrogen desorption behavior for liquid-metal cells (e.g., Cell 4 in Table 2) that contained a mixture of lithium (1.29 g) and calcium (0.11 g), i.e., 7.86 wt.% of calcium at four temperatures (267-674°C). The difference in the integrated amount of hydrogen at the various temperatures indicates the temperature dependence of hydrogen solubility. However, the result at the lowest temperature (267°C) does not show the expected profile (Fig. 6). We assume that this behavior is caused by slow hydrogen penetration through the vanadium capsules at low temperatures. Even after 756 h at 267°C, the specimen had not reached the equilibrium partial pressure of hydrogen.

Hydrogen degassing from the tantalum furnace for 900 s at temperatures between 260 and 600°C was almost constant, 3200-3300 mm³. Figure 7 shows results for liquid lithium and two lithium-calcium alloys and the temperature dependence of the solubility of hydrogen in lithium from the literature [10]. Figure 8 shows the combined results for lithium, lithium-calcium, and V-4Cr-4Ti obtained from this study. When we compare the solubility of hydrogen in liquid metals with that in V-4Cr-4Ti (Fig. 8), we can obtain the hydrogen distribution ratio between liquid lithium or Li-Ca alloys and V-4Cr-4Ti. The hydrogen distribution between a liquid-metal coolant and the structural material is an essential factor in the design of fusion reactors. Figure 9 indicates that the hydrogen distribution ratio *R* between liquid lithium or lithium-calcium alloys and V-4Cr-4Ti decreases with temperature; *R* ≈ 10 and 100 at 700 and 250°C, respectively.

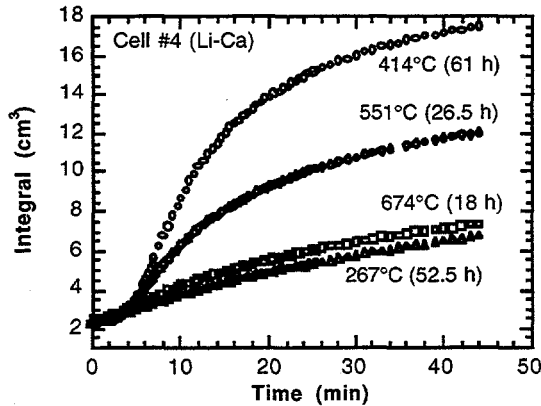


Figure 6.
Typical integrated amount of hydrogen degassed versus time for Li-7.86 wt.% Ca at temperatures between 267 and 674°C

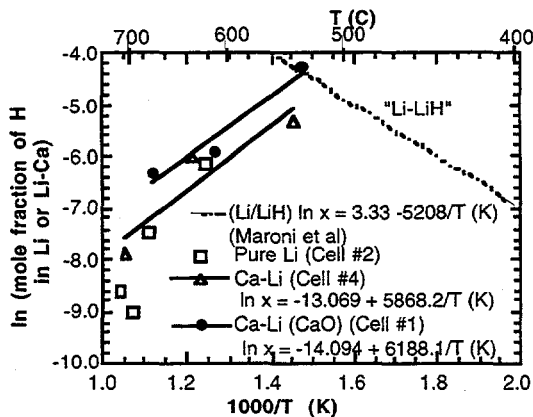


Figure 7.
ln mole fraction of H in Li, Li-Ca and Li-LiH [10] versus reciprocal temperature

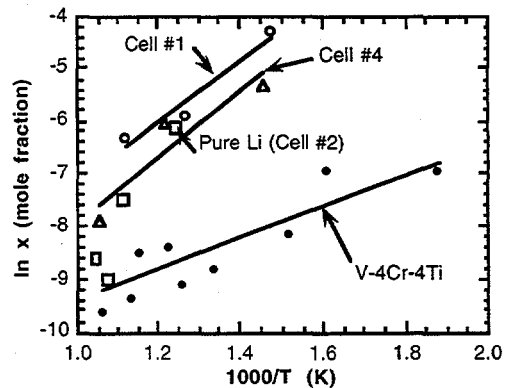


Figure 8.
ln mole fraction of H in Li, Li-Ca, and V-4Cr-4Ti versus reciprocal temperature

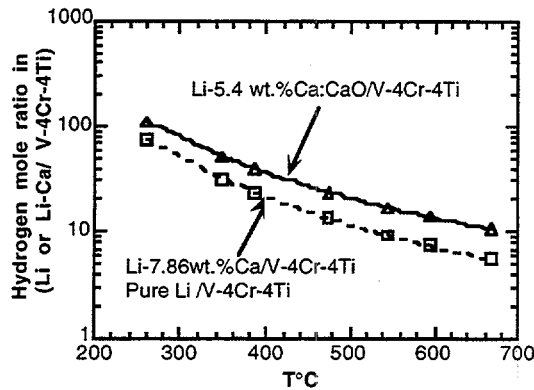


Figure 9.
Hydrogen molar distribution ratio between in Li and Li-Ca and in V-4Cr-4Ti versus temperature

CONCLUSIONS

An in-situ experimental method was developed to determine hydrogen solubility and hydrogen desorption rate in a vanadium-base alloy and liquid lithium-calcium alloys at MFR temperatures and hydrogen partial pressures. The solubility of hydrogen in V-4Cr-4Ti and liquid lithium-calcium has been measured at a hydrogen pressure of 9.09×10^{-4} torr at temperatures between 250 and 700°C.

To determine the effect of oxygen impurity in a vanadium-base alloy on hydrogen solubility and desorption, oxygen-charged V-4Cr-4Ti was also investigated. Hydrogen solubility in V-4Cr-4Ti and liquid lithium decreased with temperature. Oxygen in V-4Cr-4Ti increases hydrogen solubility and desorption kinetics. Hydrogen solubility in a Li-8 wt.% Ca alloy was also measured.

The ratio R for the distribution of hydrogen between liquid lithium or lithium-calcium alloys and V-4Cr-4Ti increases as temperature decreases ($R \approx 10$ and 100 at 700 and 250°C, respectively). However, at temperatures $< 267^\circ\text{C}$, solubility data could not be obtained by this method because of the slow kinetics of hydrogen permeation through the vanadium alloy. The measured desorption rate of hydrogen in V-4Cr-4Ti is a thermally activated process; the activation energy is 0.067 eV.

ACKNOWLEDGMENTS

C. Konicek sealed the liquid-metal cells by TIG welding. S. Crossley participated as a student in the summer research program, and F. Deleglise participated as a U.S./France foreign exchange student.

REFERENCES

- [1] J.-H. Park, G. Dragel, R. Erck, and D. L. Smith, *Solubility and Desorption of Hydrogen in V-4Cr-4Ti and Lithium*, in Fusion Materials, pp. 240-243, DOE/ER-0313/19 (1995).
- [2] J.-H. Park, D. Kupperman, and E.-T. Park, *Mechanical Properties of and Phase Transformation in V-Cr-Ti-O Solid Solutions*, in Elevated Temperature Coatings: Science and Technology II, N. B. Dahotre and J. N. Hampikian, eds., p. 323, The Minerals, Metals, and Materials Society (1996).
- [3] J. Volkl and G. Alefeld, in Topics in Applied Physics: Vol. 28, *Hydrogen in Metals I, Basic Properties*, G. Alefeld and J. Volkl, eds., Chap 12, p. 321, Springer-Verlag, Berlin, Heidelberg, New York (1978).
- [4] J. Volkl and G. Alefeld, in *Diffusion in Solids, Recent Developments*, A. S. Nowick and J. J. Burton, eds, p. 231, Academic Press, New York (1975).
- [5] R. Cantelli, F. M. Mazzolai, and M. Nuovo, *J. Phys. Chem. Solids* **31**, 1811 (1970).

- [6] N. Bose and H. Zuchner, *Z. Naturforsch* **31a**, 760 (1976).
- [7] B. Y. Liaw, G. Deublein, and R. A. Huggins, *J. Electrochem. Soc.*, **142**(7) 2196 (1995).
- [8] J.-H. Park, *Intermetallic and Electrical Insulator Coatings on High-Temperature Alloys in Liquid-Lithium Environments*, *Elevated Temperature Coatings: Science and Technology I*, N. B. Dahotre, J. N. Hampikian, and J. J. Stiglich, eds., p. 227, The Minerals, Metals, and Materials Society (1995).
- [9] A. M. Brass and A. Chanfreau, *Acta Metal.* **44**(9) 3823 (1996).
- [10] N. Rumbaut, F. Casteels, M. Brabers, *Thermodynamic Potential of Nitrogen, Carbon, Oxygen, and Hydrogen in Liquid Lithium and Sodium*, in *Material Behavior and Physical Chemistry in Liquid Metal Systems*, H. U. Borgstedt, ed., p. 437, Plenum Press, New York and London (1981).